Journal of Statistical Physics, Vol. 36, Nos. 3/4, 1984

Correlations and Spectra of an Intermittent Chaos Near Its Onset Point

Byon Chol So,[1] Nobuyuki Yoshitake,[1] Hisao Okamoto,[1] and Hazime Mori[1]

Received November 3, 1983

A one-parameter family of piecewise-linear discontinuous maps, which bifurcates from a periodic state of period m, ($m = 2, 3,...$) to an intermittent chaos, is studied as a new model for the onset of turbulence via intermittency. The onset of chaos of this model is due to the excitation of an infinite number of unstable periodic orbits and hence differs from Pomeau–Manneville's mechanism, which is a collapse of a pair of stable and unstable periodic orbits. The invariant density, the time-correlation function, and the power spectrum are analytically calculated for an infinite sequence of values of the bifurcation parameter β which accumulate to the onset point β_c from the chaos side $\varepsilon \equiv \beta - \beta_c > 0$. The power spectrum near $\varepsilon = 0$ is found to consist of a large number of Lorentzian lines with two dominant peaks. The highest peak lies around frequency $\omega = 2\pi/m$ with the power-law envelope $1/|\omega - (2\pi/m)|^4$. The second-highest peak lies around $\omega = 0$ with the envelope $1/|\omega|^2$. The width of each line decreases as ε, and the separation $\Delta\omega$ between lines decreases as $\varepsilon/\ln \varepsilon^{-1}$. It is also shown that the Liapunov exponent takes the form $\lambda \simeq \varepsilon/m$ and the mean lifetime of the periodic state in the intermittent chaos is given by $m\varepsilon^{-1}(\ln \varepsilon^{-1} + 1)$.

KEY WORDS: Burst; ordered motion; turbulence; ergodicity; Perron–Frobenius operator; eigenfunction expansion.

1. INTRODUCTION

One-dimensional maps provide us with useful models for the onset and the growth of turbulence.[1] For example, the quadratic map gives a model for a system which exhibits period-doubling transitions[2–4] leading to the onset of turbulence and band-splitting transitions in the turbulent regime.[3] In fact, the period-doubling transitions were observed in experiments on the Bénard

[1] Department of Physics, Kyushu University 33, Fukuoka 812, Japan.

0022-4715/84/0800-0367$03.50/0

convection.[5] One-dimensional maps also provide us with a convenient tool for describing the randomness of nonperiodic orbits on a strange attractor.[6] Thus one-dimensional maps are useful for studying turbulence. There are two quantities which give fundamental information on chaos. One is the Liapunov exponent which measures the degree of the sensitive dependence of orbits on their initial conditions. The other is the time-correlation function or the power spectrum which exhibits a measure-theoretical structure of nonperiodic orbits in phase space. Since turbulence is a chaotic ordered motion, the power spectrum is indispensable to studying the structure of turbulence.

Many works have been done on one-dimensional maps, but exact calculations of time correlations and power spectra are only a few. We shall calculate them exactly for a new one-parameter family of maps which exhibits a transition from a periodic state to an intermittent choas, and study its critical phenomena analytically.

The one-dimensional map we shall take is

$$x_{i+1} = f_{m,\beta}(x_i) = \begin{cases} x_i + (1/m), & \{0 \leqslant x_i < 1 - (1/m)\} \\ \beta\{x_i + (1/m) - 1\}, & \{1 - (1/m) \leqslant x_i \leqslant 1\} \end{cases} \quad (1.1)$$

where $i = 0, 1, 2,...,$ and $m = 2, 3,..., 0 \leqslant \beta \leqslant m$. This has two parameters m and β. Let m be fixed. Then a one-parameter family of maps is obtained. If $0 \leqslant \beta < 1$, then the map has one attractive periodic orbit of period m at $x_i = 0, 1/m,..., (m-1)/m$. If $1 < \beta \leqslant m$, however, the map is chaotic. In fact, as shown in Fig. 1, the map with $\beta > 1$ generates a nonperiodic orbit which is a sequence of periodic motions of period m interrupted by bursts

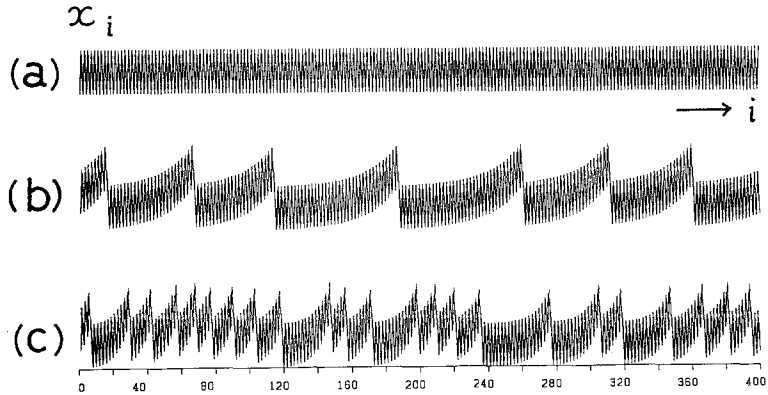

Fig. 1. Orbits x_i of the map (1.1) with $m = 3$ as functions of time i: (a) $\beta < 1$, (b) $\beta = \beta_{20} = 1.114465$, (c) $\beta = \beta_4 = 1.324718$. This indicates a transition from the periodic motion to an intermittent chaos.

irregularly. Therefore, if β is changed from below to above across $\beta = 1$, then the map undergoes a transition from the periodic state to an intermittent chaos. Indeed the main features of the nonperiodic motions shown in Fig. 1 are quite similar to the intermittent turbulence observed by Bergé *et al.* in the Bénard convection.[7] The onset of choas, however, is caused by the excitation of an infinite number of unstable periodic orbits and hence differs from the Pomeau–Manneville mechanism, which is a collapse of a pair of stable and unstable periodic orbits by a tangent bifurcation.[8,9] Therefore, the map (1.1) provides us with a new model for the onset of turbulence and associated critical phenomena. This map will be referred to as $\Psi(m, \beta)$.

The topological structure of one-dimensional maps is characterized by periodic orbits involved. It is well known that, for continuous one-dimensional maps, there exists one universal sequence for the coexistence of periodic orbits, i.e., Sarkovskii's sequence[10]

$$\begin{aligned} &3 \vdash 5 \vdash 7 \vdash 9 \vdash \cdots \\ &\vdash 2^n \times 3 \vdash 2^n \times 5 \vdash 2^n \times 7 \vdash 2^n \times 9 \vdash \cdots \\ &\vdash 2^{m+1} \vdash 2^m \vdash \cdots \vdash 2^3 \vdash 2^2 \vdash 2 \vdash 1 \end{aligned} \tag{1.2}$$

where $n = 0, 1, 2, \ldots$ and $i \vdash j$ means that if the map has a periodic orbit of period i, then the map also has a periodic orbit of period j. On the other hand, for discontinuous maps, such a universal sequence does not exist. Each one-parameter family of (1.1), however, seems to have a unique sequence of periodic orbits. In fact, we shall find such a sequence for each of $\Psi(2, \beta)$ and $\Psi(3, \beta)$ in Section 2.

In Section 3, we review a method for calculating the time correlations and power spectra.[11–13] In Section 4, we carry out the calculation for $\Psi(2, \beta)$ and $\Psi(3, \beta)$ in the chaotic regime. In Section 5, we study the asymptotic properties of the Liapunov exponent and power spectra in the vicinity of the onset point $\beta = 1$. Section 6 is devoted to some remarks.

2. SEQUENCES OF PERIODIC ORBITS FOR $\Psi(m, \beta)$

It turns out that the one-parameter families of maps (1.1) have the following sequences for the coexistence of periodic orbits. For $\Psi(2, \beta)$, $(m = 2)$,

$$\begin{aligned} &1 \vdash 4 \vdash 6 \vdash 3 \vdash 8 \vdash 10 \vdash \cdots \\ &\vdash 2n + 1 \vdash 2(2n + 1) + 2 \vdash 2(2n + 1) + 2 \cdot 2 \vdash \cdots \vdash 2 \end{aligned} \tag{2.1}$$

where $n = 0, 1, 2, \ldots$. For $\Psi(3, \beta)$ $(m = 3)$,

$$1 \vdash 6 \vdash 4 \vdash$$
$$2 \vdash 9 \vdash 7 \vdash 12 \vdash 10 \vdash 15 \vdash \cdots$$
$$\vdash 3n + 2 \vdash 3(3n + 2) + 3 \vdash 2(3n + 2) + 3 \vdash 3(3n + 2) + 3 \cdot 2$$
$$\vdash 2(3n + 2) + 3 \cdot 2 \vdash 3(3n + 2) + 3 \cdot 3 \vdash \cdots \vdash 3 \tag{2.2}$$

If $\beta < 1$, then there exists only one periodic orbit of period m and it is stable. If $\beta > 1$, however, there coexist an infinite number of periodic orbits and they are all unstable. Near $\beta = m$, periodic orbits of all periods are excited. As β is reduced from m to 1, however, periodic obits disappear successively following the sequence (2.1) or (2.2) from above. All periods except m disappear at $\beta = 1$. This gives the mechanism of the growth of chaos in terms of periodic orbits.

Table I. Values of $\{\beta_n\}$

n	β_n	m_n[a] $(m = 2)$	m_n $(m = 3)$
1	1.6180339887	3	5
2	1.4655712318	5	8
3	1.3802775690	7	11
4	1.3247179572	9	14
5	1.2851990332	11	17
6	1.2554228710	13	20
7	1.2320546314	15	23
8	1.2131497230	17	26
9	1.1974914335	19	29
10	1.1842763223	21	32
11	1.1729507500	23	35
12	1.1631197906	25	38
13	1.1544935507	27	41
14	1.1468540421	29	44
15	1.1400339374	31	47
20	1.1144648799	41	62
30	1.0854496045	61	92
39	1.0704058850	79	119

[a] $m_n \equiv mn + (m - 1)$.

Let us consider the subsequence of periods

$$m_n \equiv mn + (m-1) \qquad (n = 1, 2, 3, \ldots) \tag{2.3}$$

in each of the sequences (2.1) and (2.2). Periodic orbits of period m_n exist if and only if $\beta > \beta_n$, where β_n is the positive root of the algebraic equation

$$\beta^{n+1} - \beta^n - 1 = 0 \tag{2.4}$$

For several n's, β_n is tabulated in Table I. The $\{\beta_n\}$ is a strictly decreasing sequence to $\beta_\infty = 1$.

The minimal orbit of period m_n is a periodic orbit of type $(L^{m-1}R)^n L^{m-2}R$, where L and R indicate periodic points on the left and the right branch of (1.1), respectively. The β_n is the value of β at which this orbit passes through the vertex $x_v \equiv 1 - m^{-1} - \varepsilon$ $(\varepsilon \to 0_+)$ so that

$$f_{m,\beta}^{(m_n-1)}(1) = x_v, \qquad f_{m,\beta}(x_v) = 1 \tag{2.5}$$

in the limit $\varepsilon \to 0_+$, where $f^{(i)}$ denotes the ith iterate of f. This orbit also passes through the point $f_{m,\beta}^{(-1)}(1/m)$, where $f^{(-1)}$ denotes the inverse of f. Figures 2a and 2b show such orbit of period 5 of $\Psi(2, \beta)$ and of $\Psi(3, \beta)$, respectively.

The subsequence (2.3) will be called the main sequence. We shall calculate the correlations and spectra at $\beta = \beta_n$, where (2.4) gives

$$1/n = \ln \beta / |\ln(\beta - 1)| \tag{2.6}$$

3. CORRELATIONS AND SPECTRA

Let us consider an orbit $\{x_i\}$ generated by a map $f(x)$;

$$x_i = f(x_{i-1}) = f^{(i)}(x_0) \tag{3.1}$$

where $f^{(i)}(x) = f(f^{(i-1)}(x))$. Let us assume that $f(x)$ is ergodic in the interval $I \equiv [0, 1]$, which is satisfied by the map (1.1) in the chaotic regime $\beta > 1$.[14] Then, for almost all initial points, the orbit $\{x_i\}$ is nonperiodic and covers I densely so that the long-time average of a function $g(x_i)$ can be replaced by the space average as

$$\langle g(x) \rangle = \int_0^1 dx\, P^*(x)\, g(x) = \lim_{N \to \infty} \frac{1}{N} \sum_{i=0}^{N-1} g(x_i) \tag{3.2}$$

where $P^*(x)$ is the invariant density independent of x_0. The invariant density satisfies

$$\{HP^*\}(x) = P^*(x) \tag{3.3}$$

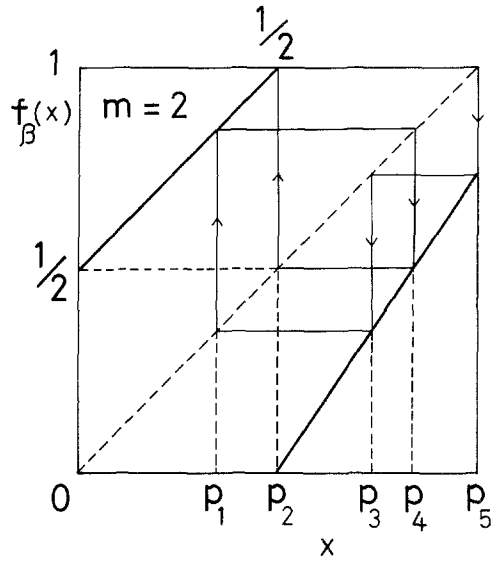

(a)

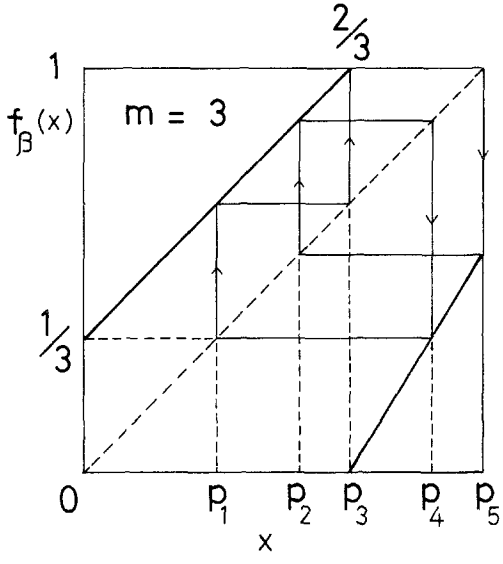

(b)

Fig. 2. Periodic orbit of period 5 for the map (1.1): (a) $m=2$, $\beta=\beta_2=1.465571$, (b) $m=3$, $\beta=\beta_1=(1+\sqrt{5})/2$.

in terms of the Perron–Frobenius operator H,

$$\{Hg\}(x) \equiv \int_0^1 dy \delta(x - f(y))\, g(y) = \sum_{y_i;\, f(y_i)=x} g(y_i)/|f'(y_i)| \tag{3.4}$$

where the summation is taken over all y_i's satisfying $f(y_i) = x$. Equation (3.3) indicates that the invariant density $P^*(x)$ is the eigenfunction of H with eigenvalue unity.

Let us now consider the time-correlation function

$$C_t(g, h) \equiv \langle g(f^{(t)}(x))\, h(x) \rangle \qquad (t = 0, 1, 2, \ldots) \tag{3.5}$$

It is convenient to introduce a modified Perron–Frobenius operator $\hat{H}$ by[11]

$$\{\hat{H}g\}(x) \equiv \frac{1}{P^*(x)} \{H(P^*g)\}(x) \tag{3.6}$$

Then (3.5) can be written as

$$C_t(g, h) = \langle g \mid \hat{H}^t h \rangle \tag{3.7}$$

where

$$\langle g \mid h \rangle \equiv \int_0^1 dx\, P^*(x)\, g(x)\, h(x) \tag{3.8}$$

In particular the normalized time-correlation function of nonperiodic orbits takes the standard form

$$\xi_t \equiv \frac{C_t(\delta x, \delta x)}{C_0(\delta x, \delta x)} = \frac{\langle \delta x \mid \hat{H}^t\, \delta x \rangle}{\langle \delta x \mid \delta x \rangle} \qquad (t = 0, 1, 2, \ldots) \tag{3.9}$$

where $\delta x \equiv x - \langle x \rangle$.

Let $\psi_l(x)$ be the eigenfunction of $\hat{H}$ with an eigenvalue ν_l;

$$\hat{H}\psi_l = \nu_l \psi_l, \qquad l = 0, 1, 2, \ldots \tag{3.10}$$

which is related to the eigenfunction of H by $H(P^*\psi_l) = \nu_l(P^*\psi_l)$. Since $f(x)$ is ergodic, $\nu_0 = 1$ is nondegenerate with ψ_0 being a nonzero constant.[11] Furthermore,[11]

$$|\nu_l| \leqslant 1, \qquad \nu_l \neq 1, \qquad \langle \psi_l \rangle = 0 \qquad \text{for} \quad l \geqslant 1 \tag{3.11}$$

This enables us to expand $\delta x \equiv x - \langle x \rangle$ in terms of ψ_l as

$$\delta x = \sum_{l=1}^{\infty} b_l \psi_l \tag{3.12}$$

Then we have $\hat{H}^t \delta x = \sum_{l=1}^{\infty} b_l v_l^t \psi_l$. Therefore the correlation function (3.9) takes the form

$$\xi_t = \sum_{l=1}^{\infty} \tilde{b}_l v_l^t \qquad (t \geqslant 0) \tag{3.13}$$

where $\tilde{b}_l = b_l \langle x \mid \psi_l \rangle / \langle \delta x \mid \delta x \rangle$, $\sum_{l=1}^{\infty} \tilde{b}_l = 1$. Therefore ξ_t is obtained analytically if one can find the eigenfunction expansion (3.12). Such simple examples were given elsewhere.[11]

In order to define the power spectrum $S(\omega)$, let us introduce

$$\delta \hat{x}_N(\omega) \equiv \sum_{t=0}^{N} \delta x_t \exp(-i\omega t) \tag{3.14}$$

Then the Wiener–Khinchin theorem leads to

$$S(\omega) \equiv \frac{1}{\langle \delta x \mid \delta x \rangle} \lim_{N \to \infty} \frac{1}{(N+1)} \langle | \delta \hat{x}_N(\omega) |^2 \rangle = \sum_{t=-\infty}^{\infty} \xi_t \exp(-i\omega t) \tag{3.15}$$

which has the following properties:

$$S(\omega) = S(-\omega), \qquad S(\omega) = S(\omega + 2\pi n), \qquad \{1/(2\pi)\} \int_0^{2\pi} S(\omega)\, d\omega = 1 \tag{3.16}$$

where n is an integer. Using $\xi_{-t} = \xi_t$ and (3.13), we finally obtain

$$S(\omega) = \left[\sum_{l=1}^{\infty} \tilde{b}_l / \{1 - v_l \exp(-i\omega)\} + \text{c.c.} \right] - 1 \tag{3.17}$$

Since $v_l = |v_l| \exp(i\omega_l)$, each term of (3.17) gives a Lorentzian spectral line at $\omega = \omega_l$ with a width $\gamma_l \equiv -\ln |v_l|$.

There are, however, three anomalous cases in which the line shape deviates from the Lorentzian. One is the degenerate case where more than two eigenvalues become identical.[11] The second is the critical case where the damping constant γ_l $(l \neq 0)$ become zero.[12,13] The third is the case where the shape of the envelope of a large number of Lorentzian lines becomes to obey a power law. In fact the last two cases occur in our map near the onset point $\beta = 1$, as will be shown later.

4. CALCULATION OF THE CORRELATIONS AND SPECTRA FOR $\Psi(m, \beta)$

A method of calculating the autocorrelations $\{\xi_n\}$ and the power spectrum $S(\omega)$ will be summarized by taking $\Psi(3, \beta)$, which may be written, for $\beta > 1$, as

$$f_\beta(x) = \begin{cases} x + (1/3), & (0 \leqslant x \leqslant 2/3) \\ \beta\{x - (2/3)\}, & (2/3 < x \leqslant 1) \end{cases} \tag{4.1}$$

Let us take $\beta = \beta_n$. Then (2.5) leads to

$$f_\beta^{(3n+2)}(1) = 1 \qquad (n = 1, 2, 3, \ldots) \tag{4.2}$$

and there exists a periodic orbit of period $3n + 2$ which passes through the vertex. The coordinates of this cycle are denoted by $\{p_1, p_2, \ldots, p_{3n+2}\}$ with $p_i < p_{i+1}$. As shown in Fig. 2, the cycle divides the total interval $I = [0, 1]$ into $3n + 2$ subintervals $\{I_i\}$ given by

$$I_i = [p_{i-1}, p_i], \qquad i = 1, 2, 3, \ldots, 3n + 2 \tag{4.3}$$

$$\begin{array}{lll} p_0 = 0, & p_{n+1} = \beta/3, & p_{2n+2} = p_{n+1} + (1/3) \\ p_1 = \beta(\beta - 1)/3, & p_{n+2} = p_1 + (1/3), & p_{2n+3} = p_{n+2} + (1/3) \\ \quad \vdots & \quad \vdots & \quad \vdots \\ p_n = \beta^n(\beta - 1)/3 = 1/3, & p_{2n+1} = p_n + (1/3) = 2/3, & p_{3n+2} = p_{2n+1} + (1/3) = 1 \end{array} \tag{4.4}$$

It should be noted that $1/m = p_n = f_{m,\beta}(p_{m_n - 1})$ for any m.

We define the characteristic functions of the subintervals

$$E_i(x) = \begin{cases} 1 & \text{if } x \in I_i, \\ 0 & \text{if } x \notin I_i, \end{cases} \qquad i \in \{1, 2, \ldots, 3n + 2\} \tag{4.5}$$

where $\sum_{i=1}^{3n+2} E_i(x) = 1$. Substituting (4.1) into (3.4), we obtain

$$\{HG\}(x) = G\left(x - \frac{1}{3}\right)\left[1 - \sum_{i=1}^{n} E_i(x)\right] + \frac{1}{\beta} G\left[\frac{1}{\beta}\left(x + \frac{2}{3}\beta\right)\right]\left[\sum_{i=1}^{n+1} E_i(x)\right] \tag{4.6}$$

for any function $G(x)$. This leads to a closed flow of the subintervals

$$\begin{gathered} HE_1 = E_{n+1} + E_{n+2}, \qquad HE_i = E_{n+1+i} \qquad (2 \leqslant i \leqslant 2n + 1); \\ HE_{2n+k} = \beta^{-1} E_{k-1} \qquad (2 \leqslant k \leqslant n + 2) \end{gathered} \tag{4.7a}$$

which can be summarized in the matrix form as

$$H\begin{bmatrix} E_1 \\ E_2 \\ \vdots \\ E_n \\ \hline E_{n+1} \\ E_{n+2} \\ \vdots \\ E_{2n} \\ E_{2n+1} \\ \hline E_{2n+2} \\ E_{2n+3} \\ \vdots \\ E_{3n+1} \\ E_{3n+2} \end{bmatrix} = \left[\begin{array}{ccc|ccc|ccc} & & & 1 & 1 & & & & \\ & & & & 1 & & & & \\ & & & & & \ddots & & & \\ & & & & & 1 & & & \\ \hline & & & & & & 1 & & \\ & & & & & & & 1 & \\ & & & & & & & & \ddots \\ & & & & & & & & 1 \\ & & & & & & & & 1 \\ \hline \beta^{-1} & & & & & & & & \\ & \beta^{-1} & & & & & & & \\ & & \ddots & & & & & & \\ & & \beta^{-1} & & & & & & \\ & & & \beta^{-1} & & & & & \end{array}\right] \begin{bmatrix} E_1 \\ E_2 \\ \vdots \\ E_n \\ \hline E_{n+1} \\ E_{n+2} \\ \vdots \\ E_{2n} \\ E_{2n+1} \\ \hline E_{2n+2} \\ E_{2n+3} \\ \vdots \\ E_{3n+1} \\ E_{3n+2} \end{bmatrix} \tag{4.7b}$$

Any subinterval flows into subintervals, covering each of the subintervals uniformly. Hence the invariant density $P^*(x)$ must be a step function given by a linear combination of the characteristic functions $E_i(x)$ as

$$P^*(x) = \sum_{i=1}^{3n+2} a_i E_i(x) \tag{4.8}$$

Since $HP^* = P^*$, the coefficients $\{a_i\}$ are found to be

$$\begin{array}{lll} & a_{n+1} = A\beta, & a_{2n+2} = A\beta \\ a_1 = A, & a_{n+2} = A, & a_{2n+3} = A \\ a_2 = A\beta^{-1}, & a_{n+3} = A\beta^{-1}, & a_{2n+4} = A\beta^{-1} \\ a_3 = A\beta^{-2}, & a_{n+4} = A\beta^{-2}, & a_{2n+5} = A\beta^{-2} \\ \vdots & \vdots & \vdots \\ a_n = A\beta^{-n+1}, & a_{2n+1} = A\beta^{-n+1}, & a_{3n+2} = A\beta^{-n+1} \end{array} \tag{4.9}$$

where $A = 3/\{(\beta-1)[(3n+2)(\beta-1)+3]\}$ from the normalization. This leads to the following average value of x_i:

$$\langle x \rangle = (1/3) + \{6 + (3-\beta)(\beta-1)\}/6\{(3n+2)(\beta-1)+3\} \tag{4.10}$$

Hence $\langle x \rangle \to 1/3$ as $\beta \searrow 1$, where (2.6) has been used. The invariant density $P^*(x)$ is shown in Figs. 3a and 3b for $\Psi(3, \beta_{20})$ and $\Psi(2, \beta_{39})$, respectively. The invariant density $P^*(x)$ consists of m_n steps, where m_n is given by (2.3) with $m = 3, 2$. It is remarkable that $P^*(x)$ has m peaks around the periodic points $x_i = 0, 1/m, \ldots, (m-1)/m$.

The Liapunov exponent $\lambda^{(11)}$ turns out to be

$$\lambda \equiv \langle \ln |f'(x)| \rangle = \frac{(n+1)(\beta-1)+1}{(3n+2)(\beta-1)+3} \ln \beta \tag{4.11}$$

In order to obtain the eigenfunction expansion of δx, it is sufficient to take the $2(3n+2)$-dimensional vector space spanned by the bases $\{E_i, xE_i;\ i \in \{1, 2, 3, \ldots, 3n+2\}\}$. Let us introduce the column vector

$$e \equiv (E_1, E_2, \ldots, E_{3n+2}, xE_1, xE_2, \ldots, xE_{3n+2})^T \tag{4.12}$$

where the superscript T indicates the transpose. Then the modified Perron–Frobenius operator $\hat{H}$ is represented by the $(6n+4) \times (6n+4)$ matrix M defined by $\hat{H}e = M^T \cdot e$. The matrix can be calculated from (3.4), (4.6), and (4.8) in a straightforward manner and turns out to take the form

$$M = \begin{bmatrix} M_{11} & M_{12} \\ M_{21} & M_{22} \end{bmatrix} \tag{4.13}$$

$$\begin{aligned} &M_{11} \equiv M(1, 1, \beta^{-1}, \beta^{-(n+1)}), && M_{12} \equiv M(2/3, -1/3, -\beta^{-1}/3, 2\beta^{-(n+1)}/3) \\ &M_{21} \equiv M(0, 0, 0, 0) = 0, && M_{22} \equiv M(\beta^{-1}, 1, \beta^{-1}, \beta^{-(n+2)}) \end{aligned} \tag{4.14}$$

in terms of the $(3n+2) \times (3n+2)$ matrix

$$M(u, v, x, y) \equiv \begin{bmatrix} & & & u & & 1 \\ & & & & \ddots & \\ & & & & u & n \\ x & & & & & y \quad n+1 \\ v & & & & & \\ & \ddots & & & & \\ & v & & & & 2n+1 \\ & & v & & & 2n+2 \\ & & & v & & \\ & & & & \ddots & \\ & & & & v & 3n+2 \end{bmatrix} \tag{4.15}$$

where the unspecified elements are all zero.

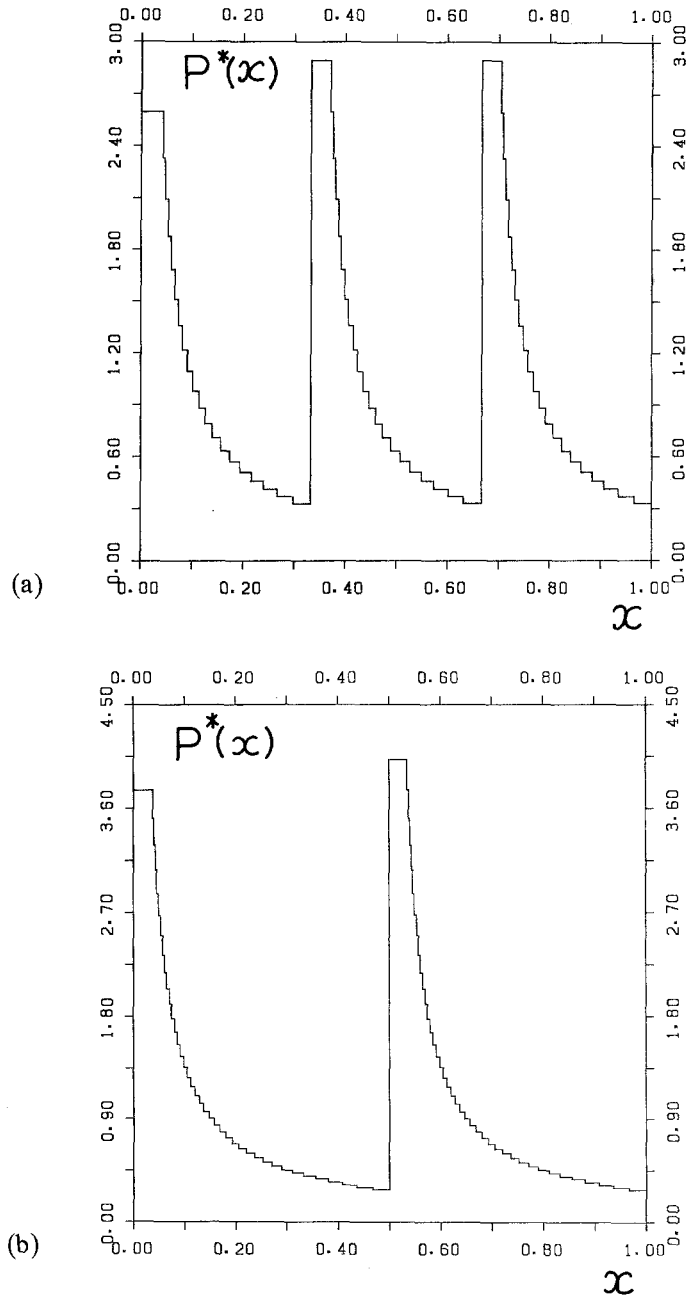

Fig. 3. Invariant density of the map (1.1): (a) $m = 3$, $\beta = \beta_{20} = 1.114465$, (b) $m = 2$, $\beta = \beta_{39} = 1.070406$.

The eigenvalues v_l of M are determined by $\det(M - vI) = 0$, i.e.,

$$\det(M_{11} - vI) = 0 \Rightarrow v^{3n+2} - \beta^{-1}v^{3n-1} - \beta^{-(n+1)} = 0 \tag{4.16a}$$

$$\det(M_{22} - vI) = 0 \Rightarrow v^{3n+2} - \beta^{-2}v^{3n-1} - \beta^{-2(n+1)} = 0 \tag{4.16b}$$

where I is the unit matrix. It follows from (2.4) that (4.16a) has one positive root $v = v_0 \equiv 1$, representing the eigenvalue of the invariant density. The roots of (4.16a) are denoted by $\{v_i\}$, $(i = 0, 1, \ldots, 3n + 1)$, and the roots of (4.16b) by $\{v_j\}$ $(j \equiv 3n + 2 + i)$. The eigenvector α_l of M with an eigenvalue v_l, $(l = i, j)$, turns out to be

$$\alpha_i = \begin{bmatrix} s_i \\ t_i \end{bmatrix} \text{ for } v_i, \qquad \alpha_j = \begin{bmatrix} s_j \\ t_j \end{bmatrix} \text{ for } v_j \tag{4.17}$$

in terms of the $(3n + 2)$-dimensional vectors,

$$s_i = \begin{bmatrix} 1 \\ v_i^{-3} \\ v_i^{-6} \\ \vdots \\ v_i^{-3(n-1)} \\ \hline v_i^{2} \\ v_i^{-1} \\ v_i^{-4} \\ v_i^{-7} \\ \vdots \\ v_i^{-3n+2} \\ \hline v_i \\ v_i^{-2} \\ v_i^{-5} \\ v_i^{-8} \\ \vdots \\ v_i^{-3n+1} \end{bmatrix}, \qquad t_i = \begin{bmatrix} 0 \\ 0 \\ 0 \\ \vdots \\ 0 \\ \hline 0 \\ 0 \\ 0 \\ 0 \\ \vdots \\ 0 \\ \hline 0 \\ 0 \\ 0 \\ 0 \\ \vdots \\ 0 \end{bmatrix} = 0, \qquad \begin{matrix} 1 \\ \\ \\ \\ n \\ \\ n+1 \\ \\ \\ \\ 2n+1 \\ \\ 2n+2 \\ \\ \\ \\ \\ 3n+2 \end{matrix} \tag{4.18a}$$

$s_j = \{1/(3\Lambda_j)\}$

$$\times \begin{bmatrix} \beta^{-(2n+1)} \\ \beta^{-(2n+1)}v_j^{-3} \\ \beta^{-(2n+1)}v_j^{-6} \\ \vdots \\ \beta^{-(2n+1)}v_j^{-3(n-1)} \\ \hline v_j^2[\beta^{-(2n+1)} - \beta\Lambda_j] \\ v_j^{-1}[\beta^{-(2n+1)} - \beta^0\Lambda_j] \\ v_j^{-4}[\beta^{-(2n+1)} - \beta^{-1}\Lambda_j] \\ v_j^{-7}[\beta^{-(2n+1)} - \beta^{-2}\Lambda_j] \\ \vdots \\ v_j^{-3n+2}[\beta^{-(2n+1)} - \beta^{-(n-1)}\Lambda_j] \\ \hline v_j[\beta^{-(2n+1)} - 2\beta\Lambda_j] \\ v_j^{-2}[\beta^{-(2n+1)} - 2\beta^0\Lambda_j] \\ v_j^{-5}[\beta^{-(2n+1)} - 2\beta^{-1}\Lambda_j] \\ v_j^{-8}[\beta^{-(2n+1)} - 2\beta^{-2}\Lambda_j] \\ \vdots \\ v_j^{-3n+1}[\beta^{-(2n+1)} - 2\beta^{-(n-1)}\Lambda_j] \end{bmatrix}, \quad t_j = \begin{bmatrix} 1 \\ (\beta v_j^3)^{-1} \\ (\beta v_j^3)^{-2} \\ \vdots \\ (\beta v_j^3)^{-(n-1)} \\ \hline \beta v_j^2 \\ \beta v_j^2(\beta v_j^3)^{-1} \\ \beta v_j^2(\beta v_j^3)^{-2} \\ \beta v_j^2(\beta v_j^3)^{-3} \\ \vdots \\ \beta v_j^2(\beta v_j^3)^{-n} \\ \hline \beta v_j \\ \beta v_j(\beta v_j^3)^{-1} \\ \beta v_j(\beta v_j^3)^{-2} \\ \beta v_j(\beta v_j^3)^{-3} \\ \vdots \\ \beta v_j(\beta v_j^3)^{-n} \end{bmatrix} \begin{matrix} 1 \\ \\ \\ \\ n \\ \\ n+1 \\ \\ \\ \\ \\ 2n+1 \\ \\ 2n+2 \\ \\ \\ \\ \\ 3n+2 \end{matrix} \tag{4.18b}$$

where $\Lambda_j \equiv v_j^{3n+2} - \beta^{-1}v_j^{3n-1} - \beta^{-(n+1)} = -\beta^{-2}(\beta - 1)(v_j^{(3n-1)} + 1)$.

The relevant eigenfunctions of $\hat{H}$ are given by the inner products of α_l and e. Therefore we obtain

$$\psi_l = \alpha_l^T \cdot e \qquad (l = i, j) \tag{4.19}$$

where the superscript T indicates the transpose and $\psi_0 = 1$. As shown in Appendix A, we have

$$(0, 0,..., 0, 1, 1,...,..., 1) = \sum_{i=0}^{3n+1} b_i\alpha_i^T + \sum_{i=0}^{3n+1} b_j\alpha_j^T \tag{4.20}$$

where $j \equiv 3n + 2 + i$, and b_i, b_j are defined by

$$b_0 = \langle x \rangle \tag{4.21a}$$

$$b_i = \frac{\beta^2[r_{1,i} + r_{2,i} + r_{3,i}]}{3(1 + v_i^{3n-1})[(3n-1)(1 - \beta^{-1}v_i^{-3}) + 3]} \qquad (i \neq 0) \tag{4.21b}$$

$$r_{1,i} \equiv \varepsilon\beta^{-1} - (\Lambda_i + \beta^{-2}\varepsilon^2)\left[1 - \frac{(\beta v_i^2)^{-1}}{\beta v_i^3 - 1}\right]$$

$$r_{2,i} \equiv \varepsilon\beta^{-2}v_i^{-2} - \beta^{-1}v_i^{-2}(\Lambda_i + \beta^{-2}\varepsilon^2)\left(1 - \frac{v_i}{\beta v_i^3 - 1}\right) + \beta^{-1}v_i^{-2}\Lambda_i \frac{1}{1 + v_i + v_i^2}$$

$$r_{3,i} \equiv \varepsilon\beta^{-2}v_i^{-1} - \beta^{-1}v_i^{-1}(\Lambda_i + \beta^{-2}\varepsilon^2)\left(1 - \frac{v_i}{\beta v_i^3 - 1}\right) + 2\beta^{-1}v_i^{-1}\Lambda_i \frac{1}{1 + v_i + v_i^2}$$

$$\Lambda_i \equiv v_i^{3n+2} - \beta^{-2}v_i^{3n-1} - \beta^{-2(n+1)} = \beta^{-2}(\beta - 1)(v_i^{3n-1} + 1)$$

$$b_j = \frac{\varepsilon^2\beta^{-2}}{(1 - \beta v_j^3)\{(3n-1)(1 - \beta^{-2}v_j^{-3}) + 3\}} \tag{4.21c}$$

with $\varepsilon \equiv \beta - 1$. Hence, using (4.20), we obtain the eigenfunction expansion

$$\delta x = \sum_{i=1}^{3n+2} xE_i - \langle x\rangle = (0, 0, \ldots, 0, 1, 1, \ldots, 1)\cdot e - \langle x\rangle$$
$$= \sum_{i=1}^{3n+1} b_i\psi_i + \sum_{i=0}^{3n+1} b_j\psi_j \tag{4.22}$$

where the $\langle x\rangle$ term canceled out the $i = 0$ term due to (4.21a). This gives (3.12) with the explicit expressions (4.21) for b_l.

Therefore the correlation function $C_t(\delta x, \delta x)$ can be written as

$$C_t(\delta x, \delta x) = \langle \delta x \mid \hat{H}^t\, \delta x\rangle = \sum_{i=1}^{3n+1} B_i v_i^t + \sum_{i=0}^{3n+1} B_j v_j^t \tag{4.23}$$

$$B_l \equiv b_l\langle x \mid \psi_l\rangle = b_l\langle x \mid \alpha_l^T \cdot e\rangle \qquad (l = i, j) \tag{4.24}$$

where

$$\langle x \mid \alpha_i^T \cdot e\rangle = \frac{1}{6[(3n+2)\varepsilon + 3]}(X + Y + Z) \tag{4.25}$$

$$X = \varepsilon^2\beta(\beta + 1)(1 + v_i^{-1} + v_i^{-2})\frac{1 - (\beta v_i^{-3})^{(n-1)}}{v_i^3 - \beta}$$

$$Y = 2\varepsilon v_i^{-1}(1 + 2v_i^{-1})\frac{1 - v_i^{-3(n-1)}}{v_i^3 - 1}$$

$$Z = \beta v_i\{(\beta + 1)v_i + (\beta + 3)\} + \varepsilon[\beta^2 + (\beta^2 + 1)v_i^{-1} + (\beta^2 + 3)v_i^{-2}]$$

$$\langle x \,|\, \alpha_j^T \cdot e \rangle = (R_1 + R_2) \tag{4.26a}$$

$$R_1 = \frac{-\beta^2}{18(1+v_j^{3n-1})[(3n+2)\varepsilon+3]}(X_1 + Y_1 + Z_1) \tag{4.26b}$$

$$X_1 = \varepsilon^2 \left[\beta + \varepsilon(\beta+1)\frac{1-(\beta v_j^{-3})^{(n-1)}}{v_j^3 - \beta}\right]$$

$$\begin{aligned} Y_1 = {} & \varepsilon v_j^{-1}[(\beta+1)v_j^3 + \varepsilon\beta^{-1}(\beta^2+1)] \\ & + \beta^{-2}(1+v_j^{3n-1})\, v_j^{-1}[v_j^3\beta^2(1+\beta) + \varepsilon(\beta^2+1)] \\ & + \varepsilon^3(\beta+1)v_j^{-4}\frac{1-(\beta v_j^{-3})^{(n-1)}}{1-\beta v_j^{-3}} \\ & + \varepsilon^2(\beta+1)\beta^{-2}(1+v_j^{3n-1})v_j^{-4}\frac{1-v_j^{-3(n-1)}}{1-v_j^{-3}} \\ & + 2\varepsilon^2\beta^{-1}v_j^{-4}\frac{1-v_j^{-3(n-1)}}{1-v_j^{-3}} \\ & + 2\varepsilon\beta^{-3}(1+v_j^{3n-1})v_j^{-4}\frac{1-(\beta^{-1}v_j^{-3})^{n-1}}{1-\beta^{-1}v_j^{-3}} \end{aligned}$$

$$\begin{aligned} Z_1 = {} & \varepsilon v_j^{-2}[(\beta+3)v_j^3 + \varepsilon\beta^{-1}(\beta^2+3)] \\ & + 2\beta^{-2}(1+v_j^{3n-1})\, v_j^{-2}[v_j^3\beta^2(\beta+3) + \varepsilon(\beta^2+3)] \\ & + \varepsilon^3(\beta+1)v_j^{-5}\frac{1-(\beta v_j^{-3})^{n-1}}{1-\beta v_j^{-3}} \\ & + 2\varepsilon^2(\beta+1)\beta^{-2}(1+v_j^{3n-1})v_j^{-5}\frac{1-v_j^{-3(n-1)}}{1-v_j^{-3}} \\ & + 4\varepsilon^2\beta^{-1}v_j^{-5}\frac{1-v_j^{-3(n-1)}}{1-v_j^{-3}} \\ & + 8\varepsilon\beta^{-3}(1+v_j^{3n-1})v_j^{-5}\frac{1-(\beta^{-1}v_j^{-3})^{n-1}}{1-\beta^{-1}v_j^{-3}} \end{aligned}$$

$$R_2 = \frac{1}{27[(3n+2)\varepsilon+3]}\{X_2 + Y_2 + Z_2\} \tag{4.26c}$$

$$X_2 = \varepsilon^2\beta^3 + \varepsilon^3\beta(\varepsilon^2+3\beta)\frac{1-(\beta v_j^{-3})^{n-1}}{v_j^3-\beta}$$

$$Y_2 = \beta^2 v_j^2(\varepsilon^2 + 3\beta) + \varepsilon v_j^{-1}[\varepsilon^4 + 3\beta(1+\beta\varepsilon)]$$
$$+ \varepsilon^3\beta(\varepsilon^2 + 3\beta)v_j^{-1}\frac{1-(\beta v_j^{-3})^{n-1}}{v_j^3 - \beta}$$
$$+ 3\varepsilon\beta^{-1}v_j^{-1}\frac{1-(\beta^{-1}v_j^{-3})^{n-1}}{v_j^3 - \beta^{-1}}$$
$$+ 3\varepsilon^2(1+\beta)v_j^{-1}\frac{1-v_j^{-3(n-1)}}{v_j^3 - 1}$$

$$Z_2 = \beta^2 v_j[\varepsilon^2 + 6(\beta+1)] + \varepsilon v_j^{-2}[\varepsilon^4 + 3(\beta+1)(2+\beta\varepsilon)]$$
$$+ \varepsilon^3\beta(\varepsilon^2 + 3\beta)v_j^{-2}\frac{1-(\beta v_j^{-3})^{n-1}}{v_j^3 - \beta}$$
$$+ 12\varepsilon\beta^{-1}v_j^{-2}\frac{1-(\beta^{-1}v_j^{-3})^{n-1}}{v_j^3 - \beta^{-1}}$$
$$+ 6\varepsilon^2(1+\beta)v_j^{-2}\frac{1-v_j^{-3(n-1)}}{v_j^3 - 1}$$

Equation (4.23) gives $\xi_t = C_t(\delta x, \delta x)/C_0(\delta x, \delta x)$ explicitly in terms of v_l and β. The eigenvalues v_l are obtained by solving the algebraic equations (4.16) numerically fo $\beta = \beta_n$. The normalized correlation function ξ_t thus obtained is shown in Fig. 4 for several cases. The fundamental period observed is $T_m = m$ $(m = 3)$.

The power spectrum $S(\omega)$ is given by (3.17) with $\tilde{b}_l = B_l/\langle \delta x \mid \delta x \rangle$, which is shown in Fig. 5 for several cases. It is remarkable that, near $\beta = 1$, $S(\omega)$ consists of many lines with two peaks; the highest peak around frequency $\Omega_m = 2\pi/m$ and the second-highest peak around $\omega = 0$. The number of lines observed in the region $0 \leqslant \omega < 2\pi$ is $m_n - 1$, and they are nearly equally spacing. As $\beta \searrow 1$, the number of lines increases as $m_n \simeq m\varepsilon^{-1} \ln \varepsilon^{-1}$ $(\varepsilon \equiv \beta - 1)$, and both of the two peaks are further enhanced.

The map $\Psi(2, \beta)$ can be treated similarly to the above. The results are summarized in Appendix B. The normalized correlation function ξ_t and the power spectrum $S(\omega)$ can be calculated from (B13) and (B9). Their explicit forms at $\beta = \beta_{39} = 1.070406$ are shown in Fig. 6a and 6b.

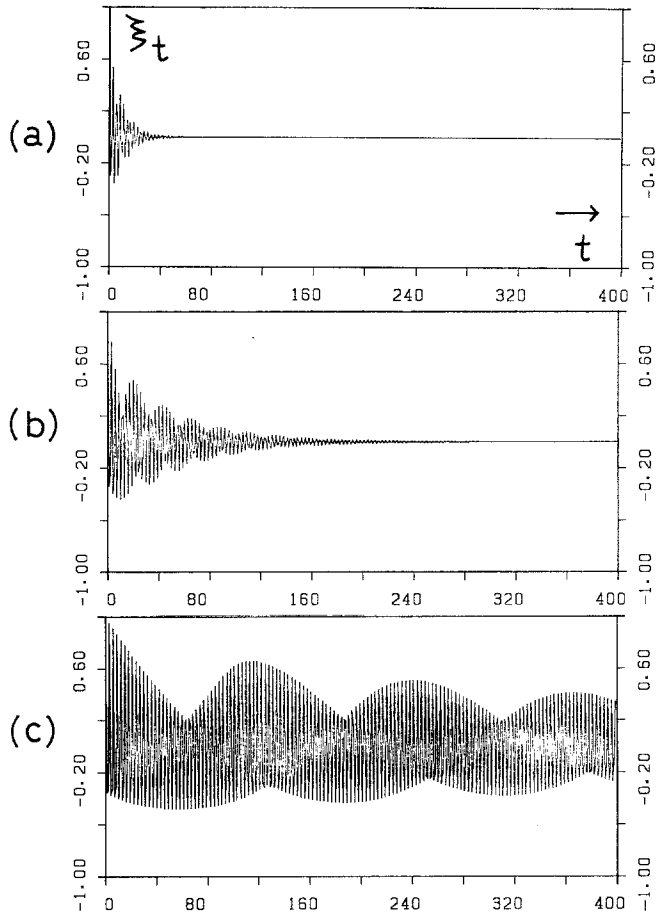

Fig. 4. Time correlation of the map $\Psi(3,\beta)$: (a) $\beta=\beta_1$, (b) $\beta=\beta_4$, (c) $\beta=\beta_{30}$.

5. CRITICAL PHENOMENA NEAR THE ONSET POINT $\beta = 1$

As $\beta \searrow 1$, (2.6) leads to $n \simeq \varepsilon^{-1} \ln \varepsilon^{-1}$ for $\varepsilon \equiv \beta - 1 \ll 1$. Then the Liapunov exponent (4.11) reduces to

$$\lambda \simeq \varepsilon/m \qquad (m=2,3) \tag{5.1}$$

The relevant eigenvalues of H satisfy (4.16), which can be generalized for arbitrary m as

$$v_i^{m_n} - \beta^{-1} v_i^{m_n - m} - \beta^{-(n+1)} = 0,\ v_j^{m_n} - \beta^{-2} v_j^{m_n - m} - \beta^{-2(n+1)} = 0 \ (\beta=\beta_n) \tag{5.2}$$

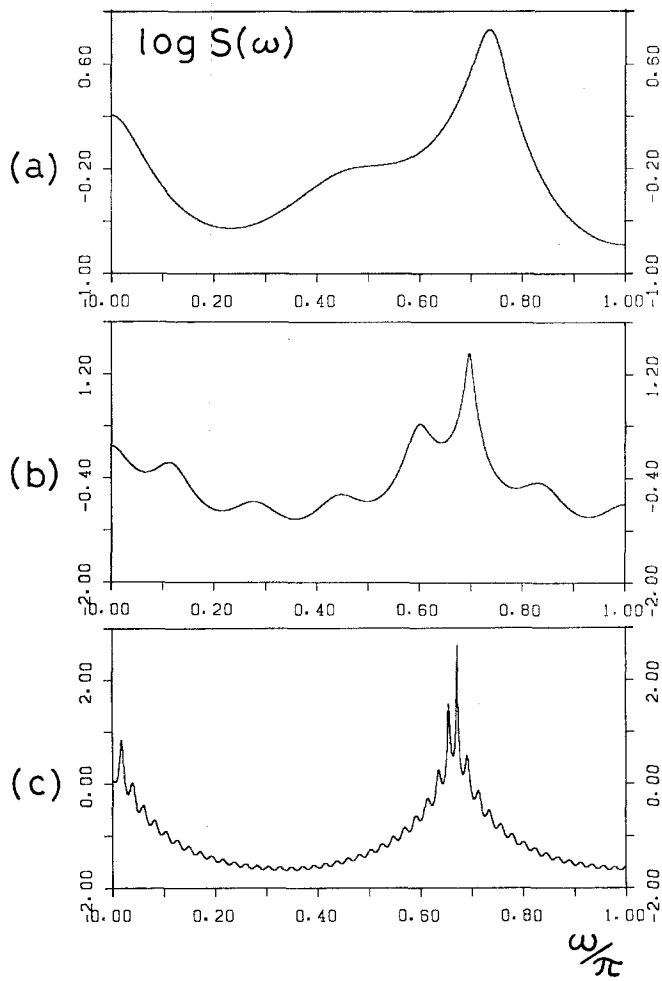

Fig. 5. Power spectum of the map $\Psi(3,\beta)$: (a) $\beta=\beta_1$, (b) $\beta=\beta_4$, (c) $\beta=\beta_{30}$.

where $j\equiv m_n+i$. The eigenvalues $\{v_i\}$ and $\{v_j\}$ for $m=3$, $m_n=92$ are shown in Fig. 7 by the asterisks and the circles, repectively. All the eigenvalues except $v_0=1$ lie inside the unit circle. Two eigenvalues of the second-largest magnitude are observed around $\arg=\pm 2\pi/3$, which are denoted by v_L and v_L^*, respectively. Indeed we have $|v_L|=0.998637$, $\arg v_L=(2\pi/3)+0.016795$. Using the argument principle and Rouche's theorem, we obtain, for $n>1$,

$$\beta^{-1}<|v_i|<1 \qquad (i\neq 0) \qquad \beta^{-1}<|v_j|<\beta^{-1/m} \tag{5.3}$$

Hence $\lim_{\beta\searrow 1}|v_i|=\lim_{\beta\searrow 1}|v_j|=1$.

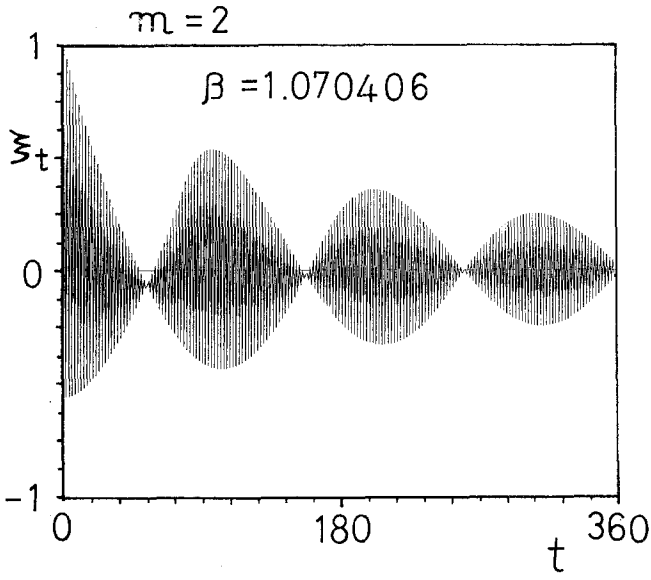

(a)

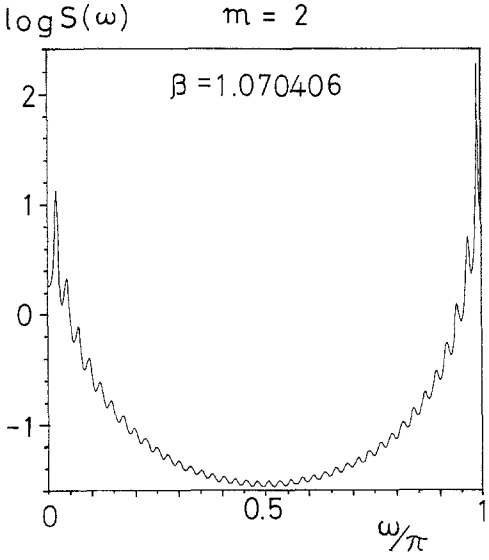

(b)

Fig. 6. (a) Correlation function and (b) power spectrum of the map $\Psi(2, \beta)$ with $\beta = \beta_{39} = 1.070406$.

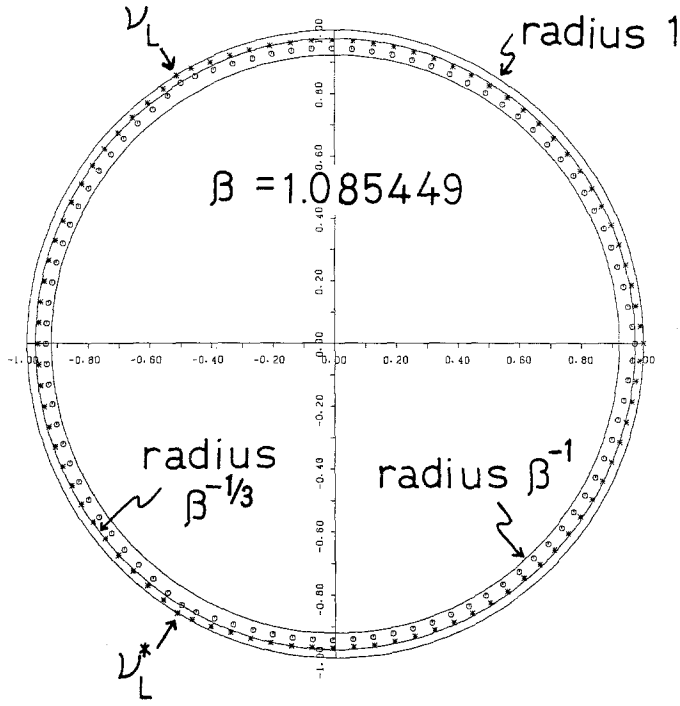

Fig. 7. Eigenvalues of the Perron–Frobenius operator for $\Psi(3, \beta_{30})$.

We now discuss this approach in more details. Let us define frequency ω_l and damping constant γ_l by

$$v_l = |v_l| \exp(i\omega_l) = \exp(-\gamma_l + i\omega_l) \tag{5.4}$$

for $l = i, j$. As observed in Fig. 7, the eigenvalues are nearly equally spacing and ω_l may be approximated as

$$\omega_l \simeq \omega_l^0 \equiv 2\pi i/m_n \qquad (i = 0, 1, \ldots, m_n - 1) \tag{5.5}$$

near $\beta = 1$, where we have numbered v_l in such a way that $0 \leqslant \omega_i < \omega_{i+1} < 2\pi$, $0 \leqslant \omega_j < \omega_{j+1} < 2\pi$. As shown in Appendix C, we obtain

$$\gamma_i \simeq (1/6n) \ln\{1 + 2\beta\varepsilon^{-2}(1 - \cos 3\omega_i)\} \qquad \text{for} \quad m = 3 \tag{5.6}$$

If ω_i is kept a constant, then this reduces to

$$\gamma_i \simeq (1/3n) \ln \varepsilon^{-1} \simeq \varepsilon/3 \tag{5.7a}$$

If the number i is fixed, then

$$\gamma_i \simeq \begin{cases} (2\pi^2/3)[\varepsilon/(\ln \varepsilon^{-1})^3]\, i^2, & \text{if } i \sim 0 \\ (2\pi^2/3)[\varepsilon/(\ln \varepsilon^{-1})^3][i-(n+1)+(1/3)]^2, & \text{if } i \sim n+1 \end{cases} \tag{5.7b}$$

$$\gamma_L \simeq (2\pi^2\varepsilon)/(3 \ln \varepsilon^{-1})^3, \qquad \text{for } i = n+1 \tag{5.7c}$$

with the corresponding frequency $\omega_i \simeq 2\pi i/(3n+2)$. These indicate that each of the spectral lines undergoes the critical slowing down. Equation (5.5) indicates that the separation between the spectral lines is given by

$$\Delta\omega \simeq 2\pi/m_n \simeq 2\pi/m\varepsilon^{-1} \ln \varepsilon^{-1} \tag{5.8}$$

As shown in Figs. 5c and 6b, the power spectrum consists of $m_n - 1$ spectral lines, which are separated by $\Delta\omega$ approximately. Each of these lines is produced by each of the eigenvalues $\{\nu_i\}$, $i \neq 0$. The spectral lines of ν_i and ν_j overlap each other. The contribution of ν_j, however, becomes zero rapidly as $\varepsilon \to 0$ and is already negligible in Figs. 5c and 6b except $\omega_j = 0$. Then the power spectrum (3.17) takes the form

$$S(\omega) = \sum_{i=1}^{m_n-1} S_i(\omega) + S_B \tag{5.9}$$

where S_B is a background spectrum. The height of the spectral line of ν_i is given by

$$S_i(\omega_i) = \frac{2B_i}{\langle \delta x \mid \delta x \rangle \gamma_i} \qquad (\gamma_i \ll 1) \tag{5.10}$$

where $\langle \delta x \mid \delta x \rangle = C_0(\delta x, \delta x) = \sum_{l=1}^{2m_n-1} B_l$. The highest peak around $\Omega_m = 2\pi/m$ is produced by the eigenvalue ν_L and its neighbors whose damping constants γ_i are small. These represent the motion of nonperiodic orbits in the neighborhood of the periodic orbit of period m, where the invariant density has dominant peaks as observed in Figs. 3a and 3b. The second-highest peak around $\omega = 0$ is produced by the eigenvalues neighboring on $\nu_0 = 1$, whose damping constants γ_i are as small as those of the neighbors of ν_L. It seems to be a general feature that the main structure of the power spectrum is thus characterized by the periodic orbit whose period is least among periodic orbits coexisting.[15]

We next consider the envelope of the highest and the second-highest peak, which is given by the ω_i dependence of (5.10). Equation (5.6) reduces to

$$\gamma_i \simeq \begin{cases} (3/2n)\,|\omega_i|^2/\varepsilon^2, & \text{if } |\omega_i| \ll \varepsilon \\ (3/2n)\,|\omega_i - (2\pi/3)|^2/\varepsilon^2, & \text{if } |\omega_i - (2\pi/3)| \ll \varepsilon \end{cases} \tag{5.11}$$

As shown in Appendix C, B_i is asymptotically given by

$$B_i \simeq \begin{cases} 1/9n^2\varepsilon^2, & \text{if } |\omega_i| \ll \varepsilon \\ 1/9^2n^2\,|\omega_i - (2\pi/3)|^2, & \text{if } |\omega_i - (2\pi/3)| \ll \varepsilon \end{cases} \tag{5.12}$$

Inserting (5.11) and (5.12) into (5.10), we obtain

$$S_i(\omega_i) \sim \begin{cases} 1/|\omega_i|^2, & \text{if } |\omega_i| \ll \varepsilon \\ 1/|\omega_i - (2\pi/3)|^4, & \text{if } |\omega_i - (2\pi/3)| \ll \varepsilon \end{cases} \tag{5.13}$$

Since $\varepsilon/\Delta\omega \sim \ln \varepsilon^{-1} \to \infty$ as $\varepsilon \to 0$, there exist a large number of spectral lines within a width of order ε. The envelope of these lines obeys (5.13). Therefore it turns out that the envelope of the highest peak obeys the power law $1/|\omega - \Omega_m|^4$ asymptotically, whereas the envelope of the second-highest peak obeys the power law $1/|\omega|^2$. It also turns out that the highest and the second-highest peak are enhanced as $\varepsilon^{-1}(\ln \varepsilon^{-1})^3$ and $\varepsilon^{-1} \ln \varepsilon^{-1}$, respectively.

We next discuss the asymptotic form of the time-correlation function ξ_t shown in Figs. 4c and 6a for $m = 3$, $n = 30$ and $m = 2$, $n = 39$, respectively. The main features of the time-correlation function consist of the following two components: a rapid oscillation with period m and a slow modulation of the amplitude with a long period around 125 and 104 for $m = 3$ and $m = 2$, respectively. These long periods are significantly different from the periods m_n of the basic cycle $(L^{m-1}R)^nL^{m-2}R$ introduced in Section 4, i.e., $m_n = mn + m - 1 = 92$ for $m = 3$, $n = 30$ and 79 for $m = 2$, $n = 39$. The two components will be shown to arise from the complex-conjugate pair of the second-largest eigenvalues,

$$\nu_L = \exp\{\pm i(\Omega_m + \hat{\omega}_L) - \gamma_L\} \tag{5.14}$$

where $\Omega_m = 2\pi/m$, $\hat{\omega}_L = 0.016795$ and 0.030328, and $\gamma_L = 0.0013637$ and 0.0030946, for $m = 3$ and 2, respectively. The contribution of (5.14) to the time-correlation function is given by the $i = L$ term of the sum (4.23) and its complex conjugate;

$$2B_L \exp(-\gamma_L t) \cos[\Omega_m(1 + \hat{q})t] \tag{5.15}$$

where we have introduced the ratio $\hat{q} \equiv \hat{\omega}_L/\Omega_m$ as the quantity analogous to the misfit of incommensurate crystalline structures.[19] If one neglects the misfit $\hat{q}$, then this leads to a simple damped oscillation with period m. The small misfit $\hat{q}$ produces a slow modulation of the amplitude whose period is given by $T_{\text{amp}} \equiv 1/\hat{q} = 124.70$ for $m = 3$ and 103.58 for $m = 2$ in agreement

with the observed periods 125 and 104, respectively. Its asymptotic form is given by

$$T_{\text{amp}} = \Omega_m/\hat{\omega}_L \simeq m\varepsilon^{-1}(\ln \varepsilon^{-1} + 1) \tag{5.16}$$

Thus the two fundamental components turn out to arise from the eigenvalues (5.14).

However, it can easily be seen that the function $\cos\{\Omega_m(1+\hat{q})t\}$ of (5.15) oscillates symmetrically in the positive and the negative direction as time t proceeds, and (5.15) never leads to the asymmetric behavior observed in Figs. 4c and 6a. This asymmetry can be obtained by adding the third-

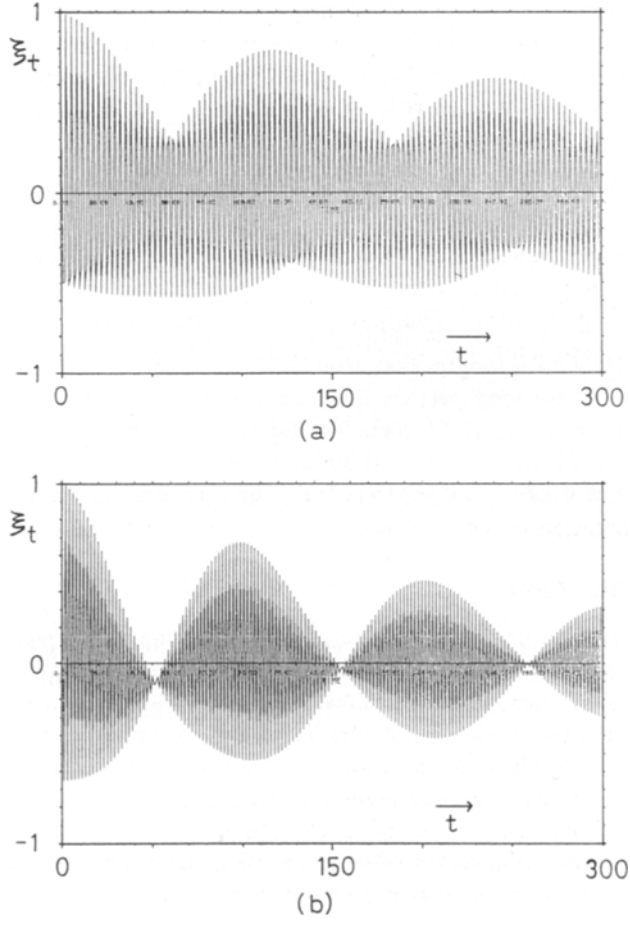

Fig. 8. Time-correlation function ξ_t calculated from (4.23) by taking only first the two largest eigenvalues (5.14) and (5.17). (a) $m=3$, $\beta=\beta_{30}$, (b) $m=2$, $\beta=\beta_{39}$.

largest eigenvalue which is given by the nearest neighbor v_n of v_L for $m = 3$ and by the nearest neighbor v_1 of $v_0 = 1$ for $m = 2$:

$$v_n = \exp[i(\Omega_3 - 0.035230) - 0.0047066]$$
$$v_1 = \exp[i \times 0.065083 - 0.0091787] \tag{5.17}$$

The time-correlation function thus obtained is shown in Figs. 8a and 8b, and turns out to reproduce Figs. 4c and 6a quite well. Thus it can be concluded that the main features of the time-correlation function are determined by the first two largest eigenvalues in (4.23), which correspond to the highest and the second-highest spectral line of the power spectrum $S(\omega)$.

The periodic state of the map is interrupted when and only when the orbit visits the subinterval I_{3n+2}. Therefore the mean lifetime τ_{per} of the periodic state is equal to the mean recurrence time of the subinterval I_{3n+2}. As shown in Appendix D, this leads to

$$\tau_{\text{per}} = 3\{\ln \varepsilon^{-1}/\ln(1+\varepsilon) + \varepsilon^{-1}\} + 2 \tag{5.18}$$

at $\beta = \beta_n$. Hence we have $\tau_{\text{per}} \simeq 3\varepsilon^{-1}(\ln \varepsilon^{-1} + 1)$ near $\beta = 1$.

It should be noted that the Liapunov exponent (5.1) does not scale as τ_{per}^{-1}. Phenomenologically the Liapunov exponent of a map can be approximated as follows. Let an orbit of a map visit the expanding region of the map n times in the mean recurrence time τ_{per} and the average slope of the map in the expanding region be α. Then the Liapunov exponent can be approximated as

$$\lambda \simeq \frac{n}{\tau_{\text{per}}} \log \alpha \tag{5.19}$$

For our map $n = (\tau_{\text{per}}/3)$ and $\alpha = 1 + \varepsilon$ so that $\lambda \simeq \varepsilon/3$, whereas for the tangent bifurcation n and α do not depend on ε so that λ scale as τ_{per}^{-1}.

6. SOME REMARKS

The time correlations and power spectra of one-parameter families of discontinuous maps which bifurcate from a periodic state of period m, $(m = 2, 3)$ to an intermittent choas have been calculated for a sequence $\{\beta_n\}$ of values of the bifurcation parameter β which accumulate to the onset point. Since the time correlations and power spectra may be assumed to be smooth functions of β except at critical points, the results obtained are valid for other values of β lying closely to $\{\beta_n\}$. On the basis of this, the asymptotic behavior of an intermittent turbulence near its onset point has been clarified.

Thus it has been found that the spectrum consists of a large number of Lorentzian lines with two dominant peaks, as shown in Figs. 5c and 6b. The highest peak has the envelope $1/|\omega - (2\pi/m)|^4$, whereas the second-highest peak has the envelope $1/|\omega|^2$. It should be noted that the exponents of the

envelope, 4 and 2, seem to be universal, irrespective of details of the model.[16] Since this is one of the most important characteristics of the intermittent turbulence, it is highly desirable to have experiments on the power spectra.

The onset of chaos of the present model is caused by the excitation of an infinite number of unstable periodic orbits accompanied by the instability of a periodic orbit of period m. Therefore the topological entropy changes from zero to positive at the onset point. This is quite different from the Pomeau–Manneville model which represents the transition from a window of period m to an observable chaos by a tangent bifurcation so that the topological entropy is already positive before the onset. This difference brings about differences in critical behavior. For example, in the Pomeau–Manneville intermittency, the mean lifetime of the periodic state is given by $\tau_{\text{per}} \sim \varepsilon^{-(z-1)/z}$, where z is the exponent of the map in the vicinity of the tangent point.[9] For piecewise-linear maps, this leads to $\tau_{\text{per}} \sim \ln \varepsilon^{-1}$ in contrast to the present model $\tau_{\text{per}} \sim \varepsilon^{-1}(\ln \varepsilon^{-1} + 1)$.[20] Furthermore, the power spectrum seems to have one dominant peaks around $\omega = 2\pi/m$ with the envelope $1/|\omega - (2\pi/m)|^2$ in contrast to the present model.[16]

It should also be noted that the tangent bifurcation at the origin could exhibit a different behavior since a fixed point at the origin represents a steady state.[4,6]

The motivation of studying simple maps like (1.1) is to know what can happen in the simplest possible maps. This is because even the simplest maps are very rich in variety of phenomena, and simple one-dimensional maps appear to describe a complex physical system, as noted in Section 1. The physical basis for this is the reduction principle that real macroscopic systems actually reduce in dimensionality.

Therefore, there arise two basic problems. One is to find a general sufficiently fine to predict all possible types of the onset of chaos and critical phenomena. The second is to find an analytic method for treating their correlations and spectra.[11,17] If a map f is not piecewise-linear, as the quadratic map $f(x) = 4ax(1-x)$ and the torus map $f(\theta) = \theta + (k/2\pi)\sin(2\pi\theta) + r$, then the relevant vector space for the eigenfunction expansion of δx is of infinite dimensions, and a new technique is needed for finding the eigenfunction expansion explicitly.

ACKNOWLEDGMENT

We would like to express our appreciation to Dr. T. Yoshida and other member of our group at Kyushu University for valuable discussions. This study was partially financed by the Scientific Research Fund of the Ministry of Education, Science and Culture.

APPENDIX A. DERIVATION OF (4.20) AND (4.21)

Let ${}^L\alpha_l$ be the left eigenvector of M with eigenvalue v_l and $X \equiv (0, 0,..., 0, 1, 1,..., 1)^T$. Let us expand X in terms of the eigenvectors α_l;

$$X = \sum_{i=0}^{3n+1} b_i \alpha_i + \sum_{i=0}^{3n+1} b_j \alpha_j \tag{A1}$$

and operate ${}^L\alpha_l$ from the left. Then we obtain

$${}^L\alpha_l \cdot X = b_l \, {}^L\alpha_l \cdot \alpha_l \tag{A2}$$

where we have used ${}^L\alpha_k \cdot \alpha_l = 0$ if $k \neq l$. This leads to

$$b_l = ({}^L\alpha_l \cdot X)/({}^L\alpha_l \cdot \alpha_l) \tag{A3}$$

The left eigenvectors are given by

$${}^L\alpha_l^T = \begin{bmatrix} {}^Ls_l \\ {}^Lt_l \end{bmatrix} \qquad (l = i, j) \tag{A4a}$$

where

$$ {}^Ls_i = \begin{bmatrix} 1 \\ N_i \\ v_i^3 N_i \\ \vdots \\ v_i^{3(n-2)} N_i \\ \hline v_i^{-2} \\ v_i^{-2} N_i \\ v_i N_i \\ v_i^4 N_i \\ \vdots \\ v_i^{3n-5} N_i \\ \hline v_i^{-1} \\ v_i^{-1} N_i \\ v_i^2 N_i \\ v_i^5 N_i \\ \vdots \\ v_i^{3n-4} N_i \end{bmatrix}, \quad {}^Lt_i = (1/3\Lambda_i) \begin{bmatrix} \beta^{-(2n+1)} & & 1 \\ \beta^{-2n} v_i^{-3n+1} \Gamma_i & & \\ \beta^{-(2n-1)} v_i^{-3n+4} \Gamma_i & & \\ \vdots & & \\ \beta^{-(n+2)} v_i^{-5} \Gamma_i & & n \\ \hline v_i^{-2} \Gamma_i & & n+1 \\ \beta^{-(2n+1)} v_i^{-3n-1} (\Gamma_i + \beta^n \Lambda_i) & & \\ \beta^{-2n} v_i^{-3n+2} (\Gamma_i + \beta^{n-1} \Lambda_i) & & \\ \beta^{-(2n-1)} v_i^{-3n+5} (\Gamma_i + \beta^{n-2} \Lambda_i) & & \\ \vdots & & \\ \beta^{-(n+2)} v_i^{-4} (\Gamma_i + \beta \Lambda_i) & & 2n+1 \\ \hline v_i^{-1} (\beta^{-2(n+1)} + 2\Lambda_i) & & 2n+2 \\ \beta^{-(2n+1)} v_i^{-3n} (\Gamma_i + 2\beta^n \Lambda_i) & & \\ \beta^{-2n} v_i^{-3n+3} (\Gamma_i + 2\beta^{n-1} \Lambda_i) & & \\ \beta^{-(2n-1)} v_i^{-3n+6} (\Gamma_i + 2\beta^{n-2} \Lambda_i) & & \\ \vdots & & \\ \beta^{-(n+1)} v_i^{-3} (\Gamma_i + 2\beta \Lambda_i) & & 3n+2 \end{bmatrix} \tag{A4b}$$

$$
{}^{L}s_j = \begin{bmatrix} 0 \\ 0 \\ 0 \\ \vdots \\ 0 \\ \hline 0 \\ 0 \\ 0 \\ 0 \\ \vdots \\ 0 \\ \hline 0 \\ 0 \\ 0 \\ 0 \\ \vdots \\ 0 \end{bmatrix} = 0, \qquad {}^{L}t_j = \begin{bmatrix} 1 & & 1 \\ N_j & & \\ (\beta v_j^3) N_j & & \\ \vdots & & \\ (\beta v_j^3)^{n-2} N_j & & n \\ \hline \beta^{-1} v_j^{-2} & & n+1 \\ (\beta v_j^3)^{-1} v_j N_j & & \\ v_j N_j & & \\ (\beta v_j^3) v_j N_j & , & \\ \vdots & & \\ (\beta v_j^3)^{n-2} v_j N_j & & 2n+1 \\ \hline \beta^{-1} v_j^{-1} & & 2n+2 \\ (\beta v_j^3)^{-1} v_j^2 N_j & & \\ v_j^2 N_j & & \\ (\beta v_j^3) v_j^2 N_j & & \\ \vdots & & \\ (\beta v_j^3)^{n-2} v_j^2 N_j & & 3n+2 \end{bmatrix} \tag{A4c}
$$

where $N_i \equiv \beta^{-(n+1)} v_i^{-3n+1}$, $N_j \equiv \beta^{-(2n+1)} v_j^{-3n+1}$, $\Gamma_i \equiv v_i^{3n+2} - \beta^{-2} v_i^{3n-1}$, $\Lambda_i \equiv v_i^{3n+2} - \beta^{-2} v_i^{3n-1} - \beta^{-2(n+1)}$. A straightforward calculation of (A.3) with (A.4) and (4.17) leads to (4.21).

APPENDIX B. RESULTS FOR $\Psi(2, \beta)$

Consider the $\Psi(2, \beta)$ map

$$
f_{2,\beta}(x) = \begin{cases} x + (1/2) & (0 \leqslant x \leqslant 1/2) \\ \beta\{x - (1/2)\}, & (1/2 < x \leqslant 1) \end{cases} \tag{B1}
$$

At $\beta = \beta_n$ there exists a periodic orbit of period $2n+1$ which passes through the vertex. This cycle divides the interval $I = [0, 1]$ into $2n+1$ subintervals $\{I_i\}$ given by

$$
\begin{aligned}
& I_i = [p_{i-1}, p_i], \qquad i = 1, 2, \ldots, 2n+1 \\
& p_0 \equiv 0 && p_{n+1} = \beta/2 \\
& p_1 = \beta(\beta - 1)/2 && p_{n+2} = p_1 + (1/2) \\
& \quad \vdots && \quad \vdots \\
& p_n = \beta^n(\beta - 1)/2 = 1/2 && p_{2n+1} = p_n + (1/2) = 1
\end{aligned} \tag{B2}
$$

Then, instead of (4.6), we obtain

$$\{HG\}(x) = G(x - 1/2)\left[1 - \sum_{i=1}^{n} E_i(x)\right] + \beta^{-1} G(\beta^{-1}(x + \beta/2))\left[\sum_{i=1}^{n+1} E_i(x)\right] \tag{B3}$$

This leads to a closed flow of the subintervals

$$\begin{gathered} HE_1 = E_{n+1} + E_{n+2}, \qquad HE_i = E_{n+1+i} \qquad (2 \leqslant i \leqslant n); \\ HE_{n+k} = \beta^{-1} E_{k-1} \qquad (1 \leqslant k \leqslant n+1) \end{gathered} \tag{B4}$$

It follows from (B4) that the invariant density $P^*(x)$ is given by

$$P^*(x) = \sum_{i=1}^{2n+1} a_i E_i(x)$$

$$a_i = A\beta^{1-i} \quad (i = 1, 2, \ldots, n), \qquad a_{n+j} = A\beta^{2-j} \quad (j = 1, 2, \ldots, n+1) \tag{B5}$$

where $A = 2/\{(\beta - 1)[(2n+1) + 2]\}$. This is shown in Fig. 3b for $n = 39$.

The Liapunov exponent turns out to be

$$\lambda = \frac{(n+1)(\beta - 1) + 1}{(2n+1)(\beta - 1) + 2} \ln \beta \tag{B6}$$

The relevant matrix representation M of $\hat{H}$ becomes

$$M = \begin{bmatrix} M_{11} & M_{12} \\ M_{21} & M_{22} \end{bmatrix}$$

$$M_{11} = M(1, 1, \beta^{-1}, \beta^{-(n+1)}), \qquad M_{12} = M(1/2, -1/2, -\beta^{-1}/2, \beta^{-(n+1)}/2)$$

$$M_{21} = M(0, 0, 0, 0) = 0, \qquad M_{22} = M(\beta^{-1}, 1, \beta^{-1}, \beta^{-(n+2)}) \tag{B7}$$

in terms of the $(2n+1) \times (2n+1)$ matrix

$$M(u, v, x, y) = \left[\begin{array}{ccc|ccc} & & & u & & \\ & & & & u & \\ & & & & & \ddots \\ & & & & & u \\ \hline x & & & & & y \\ v & & & & & \\ & v & & & & \\ & & \ddots & & & \\ & & v & & & \end{array}\right] \begin{array}{l} 1 \\ \\ \\ n \\ \\ n+1 \\ \\ \\ \\ 2n+1 \end{array} \tag{B8}$$

The eigenvalues v_l of M are determined by

$$v_i^{2n+1} - \beta^{-1} v_i^{2n-1} - \beta^{-(n+1)} = 0 \qquad (i = 0, 1, \ldots, 2n) \tag{B9a}$$

$$v_j^{2n+1} - \beta^{-2} v_j^{2n-1} - \beta^{-2(n+1)} = 0 \qquad (j = 2n+1+i) \tag{B9b}$$

The eigenvector α_l of M with eigenvalue v_l, $(l = i, j)$ is given by

$$\alpha_l = \begin{bmatrix} s_l \\ t_l \end{bmatrix}, \qquad \text{for } v_l \qquad (l = i, j) \tag{B10a}$$

$$s_i = \begin{bmatrix} 1 \\ v_i^{-2} \\ v_i^{-4} \\ \vdots \\ v_i^{-2(n-1)} \\ \hline v_i \\ v_i^{-1} \\ v_i^{-3} \\ v_i^{-5} \\ \vdots \\ v_i^{-2n+1} \end{bmatrix}, \qquad t_i = \begin{bmatrix} 0 \\ 0 \\ 0 \\ \vdots \\ 0 \\ \hline 0 \\ 0 \\ 0 \\ 0 \\ \vdots \\ 0 \end{bmatrix} \begin{matrix} 1 \\ \\ \\ \\ n \\ \\ n+1 \\ \\ \\ \\ \\ \\ 2n+1 \end{matrix} \tag{B10b}$$

$$s_j = \{1/(2\Lambda_j\} \times \begin{bmatrix} \beta^{-(2n+1)} \\ \beta^{-(2n+1)} v_j^{-2} \\ \beta^{-(2n+1)} v_j^{-4} \\ \vdots \\ \beta^{-(2n+1)} v_j^{-2(n-1)} \\ \hline v_j\{\beta^{-(2n+1)} - \beta\Lambda_j\} \\ v_j^{-1}\{\beta^{-(2n+1)} - \Lambda_j\} \\ v_j^{-3}\{\beta^{-(2n+1)} - \beta^{-1}\Lambda_j\} \\ v_j^{-5}\{\beta^{-(2n+1)} - \beta^{-2}\Lambda_j\} \\ \vdots \\ v_j^{-2n+1}\{\beta^{-(2n+1)} - \beta^{-(n-1)}\Lambda_j\} \end{bmatrix}, \qquad t_j = \begin{bmatrix} 1 \\ (\beta v_j^2)^{-1} \\ (\beta v_j^2)^{-2} \\ \vdots \\ (\beta v_j^2)^{-(n-1)} \\ \hline \beta v_j \\ \beta v_j (\beta v_j^2)^{-1} \\ \beta v_j (\beta v_j^2)^{-2} \\ \beta v_j (\beta v_j^2)^{-3} \\ \vdots \\ \beta v_j (\beta v_j^2)^{-n} \end{bmatrix} \begin{matrix} 1 \\ \\ \\ \\ n \\ \\ n+1 \\ \\ \\ \\ \\ \\ 2n+1 \end{matrix} \tag{B10c}$$

where $\Lambda_j = -\beta^{-2}(\beta - 1)(v_j^{2n-1} + 1)$.

The relevant eigenfunctions of $\hat{H}$ are given by the inner products of α_l and e;

$$\psi_l = \alpha_l^T \cdot e \qquad (l = i, j) \tag{B11}$$

where $e = (E_1, E_2, ..., E_{2n+1}, xE_1, xE_2, ..., xE_{2n+1})^T$. Then, instead of (4.21), we obtain

$$b_0 = \langle x \rangle = (1/4) + [4 + (2-\beta)(\beta-1)]/4[(2n+1)(\beta-1) + 2] \tag{B12a}$$

$$b_i = \beta^2 \{r_{1,i} + r_{2,i}\}/2(1 + v_i^{2n-1})[(2n-1)(1-\beta^{-1}v_i^{-2}) + 2] \tag{B12b}$$

$$r_{1,i} = \beta^{-1}\varepsilon - (\Lambda_i + \beta^{-2}\varepsilon^2)\left[1 - \frac{(\beta v_i)^{-1}}{\beta v_i^2 - 1}\right]$$

$$r_{2,i} = \varepsilon\beta^{-2}v_i^{-1} - \beta^{-1}v_i^{-1}(\Lambda_i + \beta^{-2}\varepsilon^2)\left(1 - \frac{v_i}{\beta v_i^2 - 1}\right) + \beta^{-1}v_i^{-1}\Lambda_i \frac{1}{1+v_i}$$

$$\Lambda_i = v_i^{2n+1} - \beta^{-2}v_i^{2n-1} - \beta^{-2(n+1)} = \beta^{-2}(\beta-1)(v_i^{2n-1} - 1)$$

$$b_j = \frac{\varepsilon^2\beta^{-2}}{(1-\beta v_j^2)[(2n-1)(1-\beta^{-2}v_j^{-2}) + 2]} \tag{B12c}$$

Thus it turns out that the time-correlation function takes the form

$$C_t(\delta x, \delta x) = \sum_{i=1}^{2n} B_i v_i^t + \sum_{i=0}^{2n} B_j v_j^t \tag{B13}$$

where $j = 2n + 1 + i$ and B_i, B_j are given by

$$B_l \equiv b_l \langle x \mid \alpha_l^T \cdot e \rangle \qquad (l = i, j) \tag{B14}$$

$$\langle x \mid \alpha_i^T \cdot e \rangle = \frac{1}{4[(2n+1)\varepsilon + 2]}\{X + Y + Z\} \tag{B15}$$

$$X = \varepsilon^2\beta(\beta+1)(1+v_i^{-1})\frac{1-(\beta v_i^{-1})^{n-1}}{v_i^2 - \beta}, \qquad Y = 2\varepsilon v_i^{-1}\frac{1 - v_i^{-2(n-1)}}{v_i^2 - 1}$$

$$Z = \beta(\beta+1)v_i + \varepsilon[\beta^2 + (\beta^2+1)v_i^{-1}]$$

$$\langle x \mid \alpha_j^T \cdot e \rangle = \{R_1 + R_2\} \tag{B16a}$$

$$R_1 = \frac{-\beta^2}{8(1+v_j^{2n-1})[(2n+1)\varepsilon + 2]}\{X_1 + Y_1\} \tag{B16b}$$

$$X_1 = \varepsilon^2 \left[\beta + \varepsilon(\beta+1)\frac{1-(\beta v_j^{-2})^{n-1}}{v_j^2-\beta}\right]$$

$$\begin{aligned} Y_1 = {} & \varepsilon v_j^{-1}[(\beta+1)v_j^2 + \varepsilon\beta^{-1}(\beta^2+1)] \\ & + \beta^{-2}(1+v_j^{2n-1})\, v_j^{-1}[v_j^2\beta^2(1+\beta) + \varepsilon(\beta^2+1)] \\ & + \varepsilon^3(\beta+1)v_j^{-3}\frac{1-(\beta v_j^{-2})^{n-1}}{1-\beta v_j^{-2}} - \varepsilon(\beta+1)\Lambda_j v_j^{-3}\frac{1-v_j^{-2(n-1)}}{1-v_j^{-2}} \\ & + 2\varepsilon^2\beta^{-1}v_j^{-3}\frac{1-v_j^{-2(n-1)}}{1-v_j^{-2}} - 2\beta^{-1}\Lambda_j v_j^{-3}\frac{1-(\beta^{-1}v_j^{-2})^{n-1}}{1-\beta^{-1}v_j^{-2}} \end{aligned}$$

$$R_2 = \frac{1}{12[(2n+1)\varepsilon+2]}\{X_2 + Y_2\} \tag{B16c}$$

$$X_2 = \varepsilon^2\beta^3 + \varepsilon^3\beta(\varepsilon^2+3\beta)\frac{1-(\beta v_j^{-2})^{n-1}}{v_j^2-\beta}$$

$$\begin{aligned} Y_2 = {} & \beta^2 v_j(\varepsilon^3+3\beta) + \varepsilon v_j^{-1}[\varepsilon^4 + 3\beta(1+\beta\varepsilon)] \\ & + \varepsilon^3\beta(\varepsilon^2+3\beta)v_j^{-1}\frac{1-(\beta v_j^{-2})^{n-1}}{v_j^2-\beta} \\ & + 3\varepsilon\beta^{-1}v_j^{-1}\frac{1-(\beta^{-1}v_j^{-2})^{n-1}}{v_j^2-\beta^{-1}} + 3\varepsilon^2(1+\beta)v_j^{-1}\frac{1-v_j^{-2(n-1)}}{v_j^2-1} \end{aligned}$$

APPENDIX C. ASYMPTOTIC FORM OF γ_i AND B_i NEAR $\beta = 1$

First we discuss the asymptotic form of $\gamma_i \equiv -\ln|v_i|$. Substituting $v_i \equiv r_i \exp(i\omega_i)$ into (4.16a) and then taking the real part, we obtain

$$\begin{aligned} & r_i^{3n-1}[(r_i^3\cos 3\omega_i - \beta^{-1})\cos(3n-1)\omega_i - r_i^3 \sin 3\omega_i \sin(3n-1)\omega_i] \\ & \quad = \beta^{-1}(\beta-1) \end{aligned} \tag{C1a}$$

Taking the imaginary part, we obtain

$$r_i^{3n-1}[r_i^3 \sin 3\omega_i \cos(3n-1)\omega_i + (r_i^3\cos 3\omega_i - \beta^{-1})\sin(3n-1)\omega_i] = 0 \tag{C1b}$$

Taking $r_i^3 = 1$ in (C1a) and (C1b), we obtain

$$r_i^{2(3n-1)} \simeq \frac{(\beta-1)^2}{\beta^2+1-2\beta\cos 3\omega_i} \tag{C2}$$

which leads to

$$\gamma_i \simeq \frac{1}{2(3n-1)} \ln[1 + 2\beta(1 - \cos 3\omega_i)/(\beta - 1)^2] \tag{C3}$$

We define $\hat{\omega}_i$ by

$$\hat{\omega}_i \equiv \begin{cases} \omega_i, & \text{if } \omega_i \sim 0 \\ \omega_i - 2\pi/3, & \text{if } \omega_i \sim 2\pi/3 \end{cases} \tag{C4}$$

If $|\hat{\omega}_i| \ll \varepsilon \equiv \beta - 1$, then (C3) leads to

$$\gamma_i \simeq 3|\hat{\omega}_i|^2/2n\varepsilon^2 \qquad (n \simeq \varepsilon^{-1} \ln \varepsilon^{-1}) \tag{C5}$$

Next we discuss the asymptotic form of B_i. Equation (5.4) leads to

$$\nu_i \simeq \begin{cases} 1 - \gamma_i + i\omega_i, & \text{if } \omega_i \sim 0 \\ [(-1 + i\sqrt{5})/2](1 - \gamma_i + i\hat{\omega}_i), & \text{if } \omega_i \sim 2\pi/3 \end{cases} \tag{C6}$$

Then it is straighforward to obtain

$$b_i \simeq \begin{cases} 1/3n\varepsilon, & \text{if } |\omega_i| \ll \varepsilon \\ -i/9n\hat{\omega}_i, & \text{if } \omega_i \sim 2\pi/3, |\hat{\omega}_i| \ll \varepsilon \end{cases} \tag{C7}$$

$$\langle x | \alpha_i^T \cdot e \rangle \simeq \begin{cases} 1/3n\varepsilon, & \text{if } |\omega_i| \ll \varepsilon \\ i/9n\hat{\omega}_i, & \text{if } \omega_i \sim 2\pi/3, |\hat{\omega}_i| \ll \varepsilon \end{cases} \tag{C8}$$

where use has been made of $\gamma_i/|\hat{\omega}_i| \simeq |\hat{\omega}_i|/\varepsilon \ln \varepsilon^{-1} \ll 1$. Therefore (4.24) leads to

$$B_i \simeq \begin{cases} 1/9n^2\varepsilon^2, & \text{if } |\omega_i| \ll \varepsilon \\ 1/9^2n^2|\hat{\omega}_i|^2, & \text{if } \omega_i \sim 2\pi/3, |\hat{\omega}_i| \ll \varepsilon \end{cases} \tag{C9}$$

which leads to (5.12).

APPENDIX D. DERIVATION OF (5.18)

At $\beta = \beta_n$, this discrete dynamical system is isomorphic to a Markov subshift among $(3n + 2)$ states. Then the mean recurrence time of the subinterval I_{3n+2} equals the inverse of the probability of I_{3n+2};[18]

$$\tau_{\text{per}} = 1 \Big/ \int_{I_{3n+2}} P^*(x)\, dx \tag{D1}$$

Using (4.4), (4.9), and (2.4), we obtain

$$\int_{I_{3n+2}} P^*(x)\,dx = A(\beta-1)^2/3 \tag{D2}$$

Therefore,

$$\tau_{\text{per}} = 3/A(\beta-1)^2 = 3n+2+[3/(\beta-1)] \tag{D3}$$

Inserting (2.6) into (D3) leads to (5.18).

REFERENCES

1. J.-P. Eckmann, *Rev. Mod. Phys.* **53**:643 (1981). H. L. Swinney, *Physica* **7D**:3 (1983).
2. R. M. May, *Nature* **261**:459 (1976).
3. S. Grossmann and S. Thomae, *Z. Naturforsch.* **32a**:1353 (1977).
4. M. J. Feigenbaum, *J. Stat. Phys.* **19**:25 (1978); *J. Stat. Phys.* **21**:669 (1979); *Phys. Lett.* **74A**:375 (1979).
5. A. Libchaber and J. Maurer, *J. Physique Coll.* C3, **41**:51 (1980); J. P. Gollub, S. V. Benson, and J. F. Stainman, *Ann. N.Y. Acad. Sci.* **375**:22 (1980); M. Giglio, S. Musazzi, and U. Perini, *Phys. Rev. Lett.* **47**:243 (1981).
6. E. N. Lorenz, *J. Atmos. Sci.* **20**:130 (1963).
7. P. Bergé, M. Dubois, P. Manneville, and Y. Pomeau, *J. Phys. Lett.* **41**:L341 (1980).
8. Y. Pomeau and P. Manneville, *Commun. Math. Phys.* **74**:189 (1980); P. Manneville and Y. Pomeau, *Physica* **1D**:219 (1980).
9. J. E. Hirsch, B. A. Huberman, and D. J. Scalapino, *Phys. Rev.* **A25**:519 (1982).
10. A. N. Sarkovskii, *Ukr. Mat. Z.* **16**:61 (1964); P. Stefan, *Commun. Math. Phys.* **54**:237 (1977).
11. H. Mori, B. C. So, and T. Ose, *Prog. Theor. Phys.* **66**:1266 (1981).
12. H. Shigematsu, H. Mori, T. Yoshida, and H. Okamoto, *J. Stat. Phys.* **30**:649 (1983).
13. T. Yoshida, H. Mori, and H. Shigematsu, *J. Stat. Phys.* **31**:279 (1983).
14. A. Lasota and J. A. Yorke, *Trans. Am. Math. Soc.* **186**:481 (1973); T.-Y. Li and J. A. Yorke, *Trans. Amer. Math. Soc.* **235**:183 (1978).
15. H. Mori, in *Nonlinear Phenomena in Chemical Dynamics*, Springer Series in Synergetics, Vol. 12 (Springer Verlag, New York, 1981), pp. 88–94.
16. K. Shobu, T. Ose, and Mori, *Prog. Theor. Phys.* **71**:458 (1984).
17. H. Fujisaka and T. Yamada, *Z. Naturforsch.* **33a**:1455 (1978).
18. J. G. Kemeny, H. Mirkil, J. L. Snell, and G. L. Thompson, *Finite Mathematical Structures* (Prentic-Hall, Englewood Cliffs, New Jersey, 1958), p. 413.
19. P. Bak, *Rep. Prog. Phys.* **45**:587 (1982).
20. J. Maurer and A. Libchaber, *J. Physique Lett.* **41**:L–515 (1980).